The Transition from Water Continuous to Oil Continuous Flow Pattern

D. P. Chakrabarti and G. Das
Dept. of Chemical Engineering, Indian Institute of Technology, Kharagpur 721302, India

P. K. Das
Dept. of Mechanical Engineering, Indian Institute of Technology, Kharagpur 721302, India

DOI 10.1002/aic.10988
Published online September 15, 2006 in Wiley InterScience (www.interscience.wiley.com).

The present study attempts to develop an objective flow pattern indicator to identify phase inversion during liquid-liquid two-phase flow through a horizontal pipe. A novel optical probe has been used for this purpose. The probability density function (PDF) analysis and the wavelet multiresolution technique have been adopted to detect the shift of phase continuity. Further attempts have been made to understand the interfacial configurations when oil is the predominant phase in the flow passage. Since little can be revealed through visualization or photography related techniques under such conditions, the information obtained from the probe signals at low phase flow rates has been exploited for this purpose. In addition, a sampling technique has been devised to verify the distribution as obtained from the probe signals. The ambivalent range between the oil-dispersed and the water-dispersed regime has been observed to be in close agreement to the empirical and analytical equations available in literature. © 2006 American Institute of Chemical Engineers *AIChE J,* 52: 3668–3678, 2006
Keywords: hydrodynamics, phase inversion, optical probe, liquid-liquid flow, signal analysis

Introduction

The simultaneous flow of two phases through a closed conduit is manifolds more complex as compared to the single phase flow of either of the fluids through the same geometry. While a single fluid can be in either laminar or turbulent flow, the two fluids can distribute themselves in a wide variety of ways, which is not under the control of the experimenter or the designer. The interfacial configurations vary with physical properties and velocities of the two fluids, the conduit geometry, its inclination, and many other operating conditions. A flow situation uniquely defined by the spatial and temporal variation of the interfacial configuration is known as flow regime or flow pattern. Several studies have been directed to the identification of flow patterns during different two-phase flow situations, with the majority of the works being confined to gas-liquid systems.

Although liquid-liquid flows are also characterized by a deformable interface, there is no guarantee that the information available for gas-liquid flows can be extended to liquid-liquid systems. There are intrinsic differences in the physics of the two flow situations. The flow of two immiscible liquids exhibits the phenomenon of phase inversion in which the dispersed phase inverts to form the continuous phase and vice versa with slight changes in the operating conditions. This has been reported in both stirred vessels as well as under flow conditions at high velocities of the two liquids. The detection of phase inversion is very important from the industrial point of view since it leads to a system with different physical behavior. In flow systems it leads to a maximum in pressure gradient,[1] thus

Correspondence concerning this article should be addressed to G. Das at gargi@che.iitkgp.ernet.in.

influencing the phase flow rates. As a result, considerable attention has been focused on the prediction of phase inversion and the ambivalent range (range of flow velocities over which phase inversion occurs). However, the majority of the studies are confined to batch processes; and in flow systems, the studies have been influenced by the information obtained from stirred vessels.[2-4]

Several researchers have proposed empirical as well as analytical equations to predict inversion. Arirachakaran et al.[5] and Yeh et al.[6] have examined the effects of liquid viscosity on the inversion point and proposed equations to predict the inversion point from the viscosities of the pure liquids. Tidhar et al.[7] have studied the influence of the surface of the mixing elements on phase inversion and concluded that the ambivalent zone is very narrow. Nädler and Mewes[8] have estimated the effect of phase inversion on the system pressure drop. Brauner and Ullmann[9] have attempted to predict the inversion point from the principle of minimization of system free energy, combined with a model to predict drop size in dense dispersions. Chesters and Issa[10] have presented a mathematical model to describe the evolution of phase inversion processes in two-fluid systems. The model has been developed within the framework of the two-fluid model for dispersed flows, using CFD techniques. The experimental identification of inversion has primarily been carried out through visual observations[5,11-14], measurement of effective conductivity of the mixture,[15-20] and estimation of pressure gradient.[20] However, no conclusive results could be obtained, primarily due to the difficulty of flow visualization at the high phase velocities.

It may further be noted that most of the world's crude oil is produced in the form of water in oil emulsions,[21-22] where a small amount of water is distributed in the oil phase. This requires a better understanding of the flow characteristics in the oil dominating regime. However, not much is known to date about the interfacial distribution under such conditions, primarily because the visualization and photography related techniques fail to discern the phase distribution at the high oil flow rates. Hapanowicz and Troniewski[23] have reported that the pressure gradient in the water dispersed in an oil flow pattern exhibits significant deviations from the predictions of the homogeneous flow model and have suggested suitable viscosity corrections to improve the predictions. They have also attempted to incorporate the influence of flow pattern in the analysis of holdup and pressure drop during liquid-liquid flow.

It is thus needless to say that further investigations are required to develop a clear understanding of the phenomenon of phase inversion. In this regard, development of a reliable technique for the detection of phase inversion would be particularly useful. In the present work, a novel optical probe based on the difference in optical properties of the two liquids is used for this purpose. Statistical analysis of the random probe signals, namely, the probability density function analysis (PDF) and the wavelet multiresolution technique, have been used to detect inversion. The signals have been compared with visual observations at low phase flow rates, and the information thus obtained is used to interpret the signals recorded at the high mixture velocities. It may be noted that past researchers[16,18,24] have referred to the oil in water distributions as the water continuous pattern and the water in oil distribution as the oil continuous regime. However, in the present study, we have referred to the oil in water patterns as the water dominant regime and the latter as the oil dominant regime to avoid confusion regarding the continuity of the phases under the different flow conditions. The dominant phase is merely the major phase in the flow passage.

Experimentation

The details of the experimental setup suitable for the study of liquid-liquid two phase flow is provided in Raj et al.[24] A schematic diagram is shown in Figure 1a. It comprises of an entry section, a test section, and an exit section in order in the direction of the flow. The test section is a circular pipe of 0.025 m diameter and 3 m in length. The entire setup is constructed of perspex to enable visualization of flow. A rectangular glass view box (VB) is attached to the test section at a distance of 2.5 meters from the entry section (ENS in Figure 1) for photography at low liquid velocities. The rectangular box has been installed to eliminate the effects of reflection and refraction by the circular cross section of the pipe.

Water and kerosene have been used as the two fluids. To distinguish between water and kerosene, the latter has been dyed with 1,4-dialkyl anthraquenone (blue). The optical probe is installed besides the view box as shown in Figure 1a. The details of the probe are provided in Jana et al.[25] It comprises of a semiconductor laser source ($\sim$2 mW, $\sim$660 nm wavelength, and 2 mm beam diameter), which serves as a source of monochromatic laser light, and a photodiode sensor (SD 3410, manufactured by Honeywell) located at the diametrically opposite point, as shown in Figure 1b. The detector is placed inside a dark box to ensure that only light from the source and not from any other agent falls on it. The diode sensor generates a DC voltage when light is incident on it. An indigenously made amplifier circuit amplifies the signal. The voltage output is recorded continuously as time series data in a computer through a data acquisition unit (Agilent 3970A) with a frequency of 23 Hz for a period of 2 min. A steady output at a constant voltage is obtained during single-phase flow of either water or kerosene through the conduit. The voltage value is higher for water due to the higher absorption coefficient of kerosene.

During two phase flow, the output is an oscillating response depending on the variations in the intensity of light incident on the photodiode. The variations depend on the fraction attenuated and scattered by the flowing medium. The amount of attenuation varies with the composition of the mixture. A higher kerosene flow rate gives a lower average value of the signal for the same flow pattern. Apart from attenuation, the narrow beam of light on its way from the source to the detector undergoes a series of different interactions, namely, reflection, refraction, absorption, scattering, and so forth, with the two phase mixture and the interfaces created by planes, waves, drops, and so on. These interactions increase the fluctuations in the signal and can also reduce the amount of light incident on the photodiode. Thus, the optical probe has been observed to be an effective tool to identify the flow patterns and the transitions on the basis of the relative proportion of the two phases in the conduit and the fraction of light scattered by the distribution of the two phases. Although the distribution varies in time and space, the output gives an insight into the gross distribution across a diametral plane. The main advantage of the probe is its non-intrusive nature, ensuring no obstruction of the flow pas-

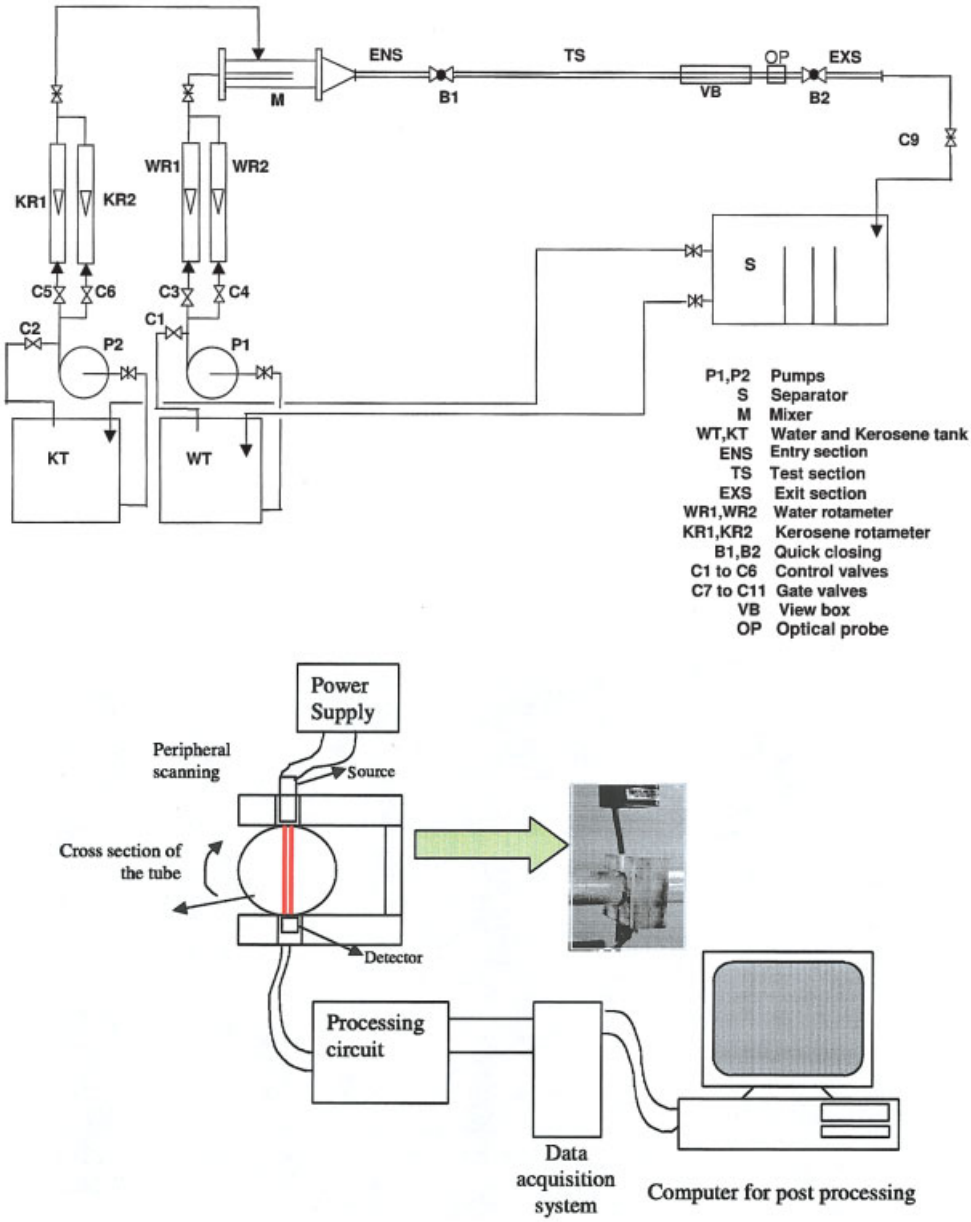

Figure 1. Experimental setup; (b) optical probe.

[Color figure can be viewed in the online issue, which is available at www.interscience.wiley.com.]

sage and no wetting of the probe with the oil phase. Moreover, the device is expected to operate under both water predominant and oil predominant flow patterns and is expected to provide an insight into the change of phase continuity with flow rates. It is also reliable, inexpensive, and provides an instantaneous response with good spatial resolution.

Statistical Analysis

Apart from visual observation of the probe signals, statistical analyses of the random signals have been performed for a better understanding of the flow phenomenon. This is particularly useful at high phase velocities where visual observation cannot reveal the flow structures. The probability density function (PDF) analysis and the wavelet transform (WT) have been adopted for this purpose. Jana et al[26] have reported considerable success in using these analyses to the conductivity probe signals for identifying the flow patterns during liquid-liquid upflow through a vertical pipe. They have presented a detailed discussion of both the techniques.

The probability density function (PDF) for a discrete random variable is a function that assigns a probability to each value of the random variable. It can be regarded as a "smoothed out" version of a histogram. The shape of the PDF serves as a useful diagnostic tool.[27] The problem of quantification of this information has been accomplished by means of the usual statistical moments (mean, variance, skewness, and kurtosis). While the mean gives us the average value of the distribution, the variance is a measure of the distribution about the mean. The

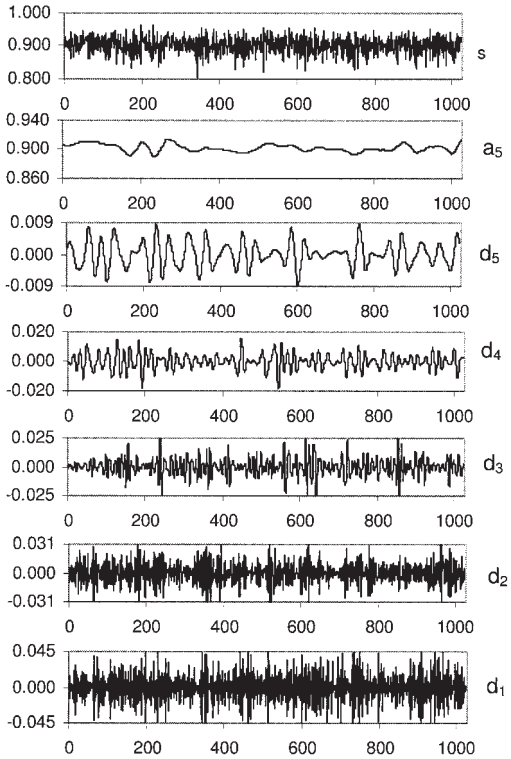

Figure 2. A full scale decomposed signal using Daubachies4 wavelet with level 5 at U_{SK} 0.06 m/s and U_{SW} 0.7 m/s.

skewness (third moment) characterizes the asymmetry of the PDF, and the kurtosis (fourth moment) characterizes the flatness of the distribution compared with the Gaussian one. The physical significance of the moments has been related to the various two-phase flow patterns by Vince and Lahey.[28]

Wavelet analysis[29-33] is a windowing technique with variable sized regions that allows long time intervals in regions where more precise low frequency information is required and short time intervals in regions where precise high-frequency information is required. This is referred to as multiresolution. The advantage of such transform, compared to the Fourier transform, manifests itself in the ability of the transform to perform local analysis. It reveals trends and discontinuities in the higher derivatives and compresses and de-noises a signal without an appreciable loss in signal energy. In fact, a signal can be decomposed to obtain a time history of the different frequency bands, which is termed as multiresolution analysis. In the present study, Daubachies 4 wavelet with level 5 is chosen as the analyzing wavelet due to its sufficient number of vanishing moments and smoothness. For all wavelet analysis, Matlab 6 with its wavelet toolbox has been utilized.

One typical signal (s) from the optical probe decomposed into five details (d_1-d_5) and one approximation (a_5) is depicted in Figure 2. In the figure, d_1 reflects the smallest scale and the highest frequency band; d_2, d_3, and so forth represent progressively lower frequency bands; and the approximation, a_5, reflects the large-scale and low frequency resolution. It is expected that the high frequency fluctuations are caused by the passage of droplets, while the large-scale low frequency fluctuations arise from a waviness of the continuous interface.

Results and Discussion

The random signals from the optical probe are recorded for different velocities of water and kerosene. The response is normalized with respect to the voltage obtained during the flow of only water through the conduit in order to facilitate a comparative study. Initially, the signals and PDF curves are compared with the photographic images at low phase velocities in the water continuous pattern. The wavelet analysis of the probe signals has provided an additional insight into the onset of dispersion or increase in interfacial waviness from the fluctuations at the different levels of the decomposed signal (d_1-d_5) and the approximation (a_5). The information obtained from the comparative study is next exploited to detect phase inversion from the quantitative measures of the histogram and the wavelet multiresolution technique. Further attempts have been made to use the statistical analysis of the random probe signals to understand the interfacial configurations in the oil dominant regime. In all the figures, U_{SW} and U_{SK} represent the superficial velocity of water and kerosene, respectively. The quantitative measures of the histogram are depicted as m (mean), σ (standard deviation), s (skewness), and k (kurtosis).

Comparison of the probe response with visual observations at low phase velocities

The random signals and the PDF curves obtained at low kerosene velocities in the water predominant pattern are presented along with the photographic observations in Figure 3. In the figure, SS and SW represent the stratified smooth and stratified wavy flow patterns, whereas P, TL, and D denote the plug, three layer, and dispersed flow patterns, respectively. A comparison of the PDF curves with photographic images shows that the stratified pattern is characterized by a smooth response at high voltage and a unimodal PDF with negligible spread. The onset of waviness at higher phase velocities is accompanied by an increase in the standard deviation of the PDF curve. It shifts to higher voltage values with increase of water velocity and vice versa for increasing kerosene flow rates, as expected. Moreover, visual observations have revealed the differences in the characteristics of the wavy interface for higher oil and water velocities. At U_{SK} = 0.06m/s, U_{SW} = 0.3m/s, the interface is characterized by a wave having low frequency and low amplitude as well as a low velocity. On the other hand, waves with an increased frequency and higher amplitudes were observed at U_{SK} = 0.3m/s, U_{SW} = 0.18m/s. The difference in the wave characteristics is probably responsible for a different sign of the skewness under the two flow conditions.

With a further increase in water velocity, the two phase mixture exhibits the plug flow pattern at low oil velocities and the three-layer flow at higher flow rates of kerosene. The plug flow pattern is characterized by intermittent kerosene chunks being intercepted by water bridges, while in the three-layer pattern the amplitude of the waves is not sufficient to reach the upper wall. They break down to form droplets that are dispersed in the interface between the two immiscible liquids. Although these are formed at higher water velocities, they are characterized by a shift of the mean response to lower voltage values and a remarkable increase in the PDF spread (as is evident from Figure 3). This arises due to the scattering of light by the droplets along with attenuation by the two-phase mix-

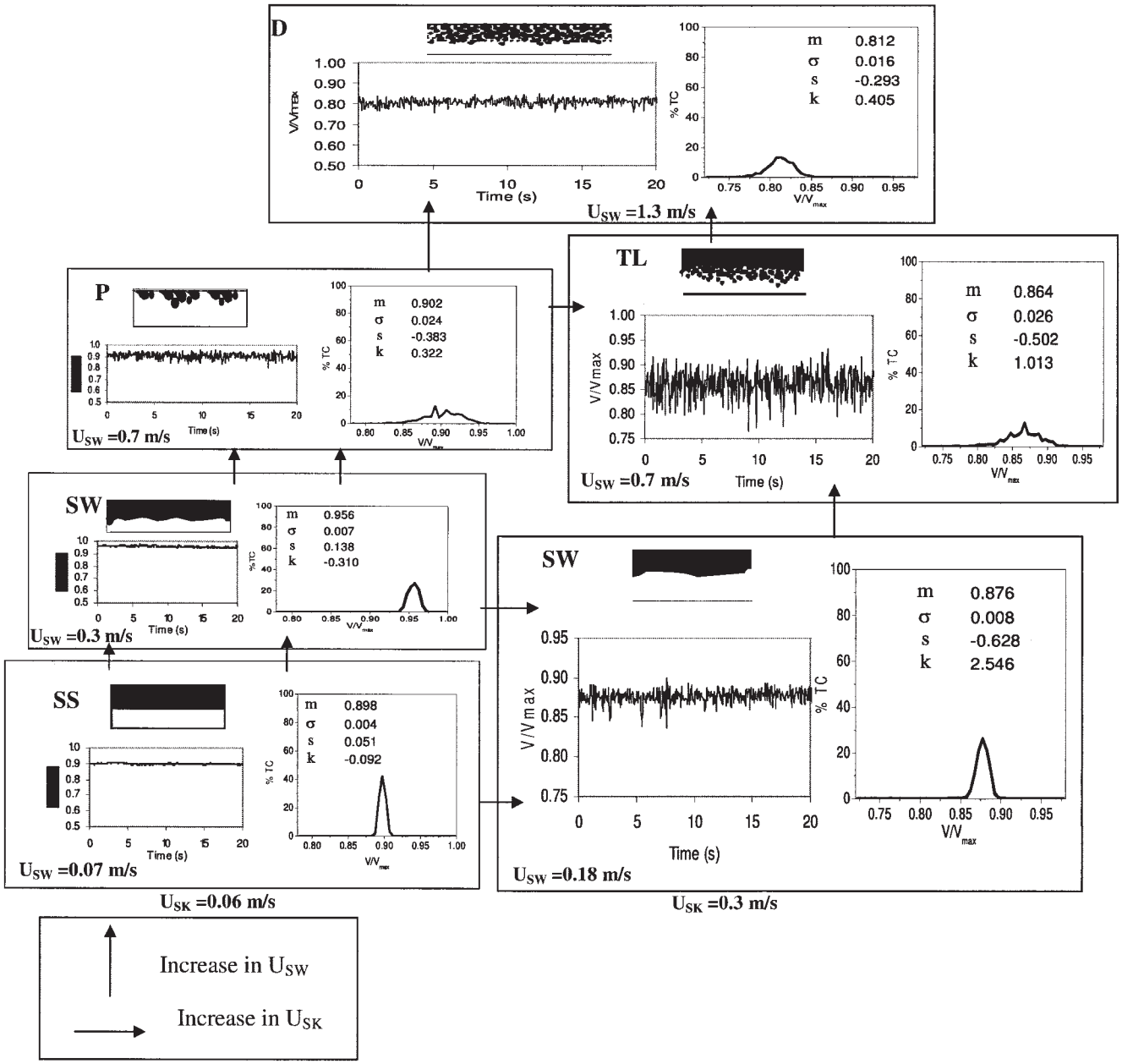

Figure 3. Description of the flow regimes at low phase velocities.

ture. The PDFs are also characterized by indentations in both the cases, unlike its smooth nature at lower water velocities.

In the dispersed flow pattern (kerosene droplets in water) at higher water velocities, the dense array of droplets propagates through the conduit at a high velocity. Their high population results in insufficient light passage. This is characterized by a decrease in the spread of the PDF and a further shift of the mean value to still lower voltages. Moreover, the PDF regains its smooth nature, thus highlighting the time invariant distribution of the dispersion at a particular cross section.

The wavelet analysis of the probe signals supplements the information provided by the PDFs. To economize the volume of communication, the results of the analysis have been represented graphically in Figure 4a and b. The graph denotes the spread in the different levels of decomposition (d_1-d_5) and the approximation (a_5) as functions of phase superficial velocity. The phase superficial velocities in Figures 3 and 4 are selected such that the mixture exhibits different flow patterns. It is evident from Figure 4 that the increased waviness in the stratified configuration is manifested by a continuous increase in oscillations at all levels, while the onset of dispersion is marked by an increase in the spread of the high frequency low resolution level (d_1). Further, the spread increases from d1-a5 for the stratified flow pattern in Figure 4a, while the reverse trend is observed for Figure 4b. This brings out the differences in the characteristics of the wavy interface for the two flow conditions and justifies the visual observation that low frequency waves traverse the interface during the stratified wavy pattern at lower phase velocities while high frequency waves mark the waviness at higher flow rates of the two phases.

The range of existence of the different flow patterns as obtained from the moments of the PDF curves is presented in Table 1. The first two moments of the PDF curves have been reported for this purpose as they have been observed to be the most effective in distinguishing between the different patterns. The table shows that there are overlap or similarity between the PDF moments obtained for the various flow patterns. For example, the stratified smooth and wavy patterns give similar values of the mean, while the plug and three layer flows have almost identical PDF spread. This is an expected result due to the inherent randomness of two-phase flow and suggests that the PDFs obtained for the different patterns might appear to be similar at first sight due to this.

Identification of phase inversion from probe signals

An interest was next felt to identify phase inversion, a unique phenomenon exhibited by liquid-liquid dispersions during which the dispersed phase inverts to form the continuous phase and vice versa under certain flow conditions. For this, the experiments are performed at increasing kerosene velocities for a constant water flow rate. The water flow rates are selected such that the pattern exhibits dispersed flow characteristics under all flow conditions. It may be noted that the distribution could be observed only at low kerosene velocities and nothing could be visualized with increase in oil flow rate (for approximately $U_{SK} \geq 0.5$ m/s).

Since identical observations have been noted for different constant water flow rates, the results have been represented for one particular water velocity ($U_{SW} = 1.3$ m/s) in Figure 5 to avoid repetition. The figure is represented in a tabular form where the different rows of the table are marked as 5.1, 5.2, and so forth. The depiction for each distribution is represented in three parts (a, b, and c) denoting the schematic and photograph of the phase distribution, the probe signals, and the corresponding PDF curves, respectively. The moments of the PDFs are also indicated for their quantification in the last column.

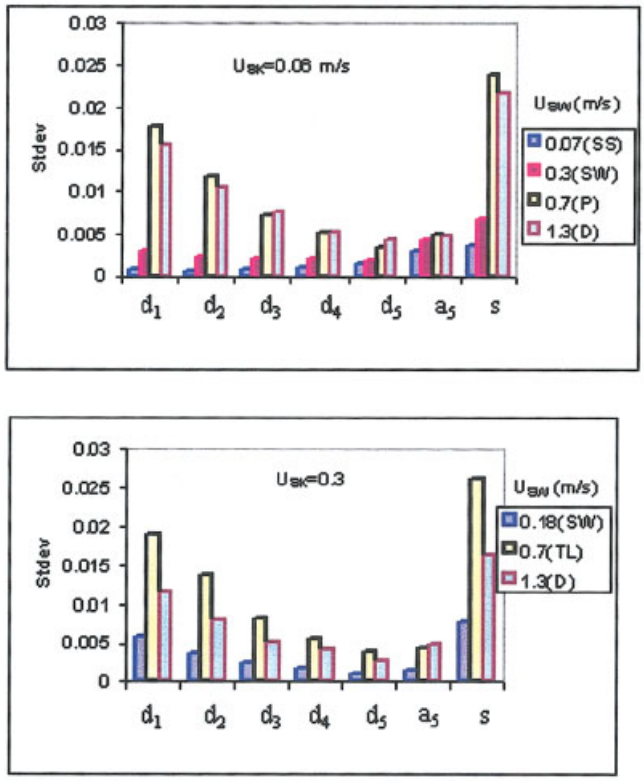

Figure 4. The spread at the different levels of the decomposed signal for (a) USK = 0.06 m/s; (b) USK = 0.3 m/s.

[Color figure can be viewed in the online issue, which is available at www.interscience.wiley.com.]

Table 1. The Range of Existence of the Different Flow Patterns as Obtained from the Moments of the PDF Curves

	m	σ
SS	≥0.9	≈0.006
SW	0.87–0.95	0.007–0.009
P	0.9–0.94	0.021–0.025
TL	0.67–0.88	0.021–0.024
D	0.72–0.86	0.013–0.022

The figure shows that at low oil velocities, the PDF is unimodal with a large spread and negative skewness. As the kerosene velocity is increased, the PDF shifts to the left, as expected. This is also accompanied by a decrease in the spread (until Figure 5.3). However, all the PDFs are skewed to the left, denoting a tendency of kerosene dispersion. As the kerosene velocity is increased further (Figure 5.4), the response exhibits a remarkable change that can be better understood from the changes in the nature of the PDF curve. The curve is characterized by a sudden increase in spread, an abrupt shift of the mean value to V/Vmax < 0.5, and a shift of the skewness to positive values. This signifies a predominance of kerosene in the flow passage. It may be noted that an identical observation has been reported by Jana et al.[24] during the transition from water predominant to the oil predominant region during liquid-liquid upflow through a vertical pipe. However, they had demonstrated that the pattern was oil dispersed in water at low oil velocities and core annular flow at high kerosene flow rates.

A further increase in kerosene velocity is marked by reduced fluctuations of the probe signals along with a shift of the PDF to still lower voltages and a further reduction in its spread. Such a change in Figure 3 indicated a dense distribution of droplets whose intense scattering resulted in the reduced spread.

The wavelet analysis was next performed for a better appraisal of the flow phenomenon. As mentioned earlier, the Daubechies 4 wavelet analysis has been used to decompose the normalized probe signals into 5 levels. For a comparative study, the oscillations at different levels of frequency (d_1-d_5), the approximation (a_5), and the main signal (s) are compared at different flow conditions. This has been shown graphically in Figure 6 where the variance from d_1-d_5, a_5, and the main signal (s) are plotted as a function of phase superficial velocities. The graph shows that the d_1 fluctuations are highest at the lowest kerosene flow rate. As the kerosene flow rate is increased, there is a slight decrease in d_1 fluctuations while the fluctuations at the other levels remain comparatively unchanged. This explains the marginal reduction in the PDF spread with increased kerosene velocity and has been attributed to the increased influence of light scattering by the dense dispersion of droplets. However, the d_1 fluctuations continue to be higher as compared

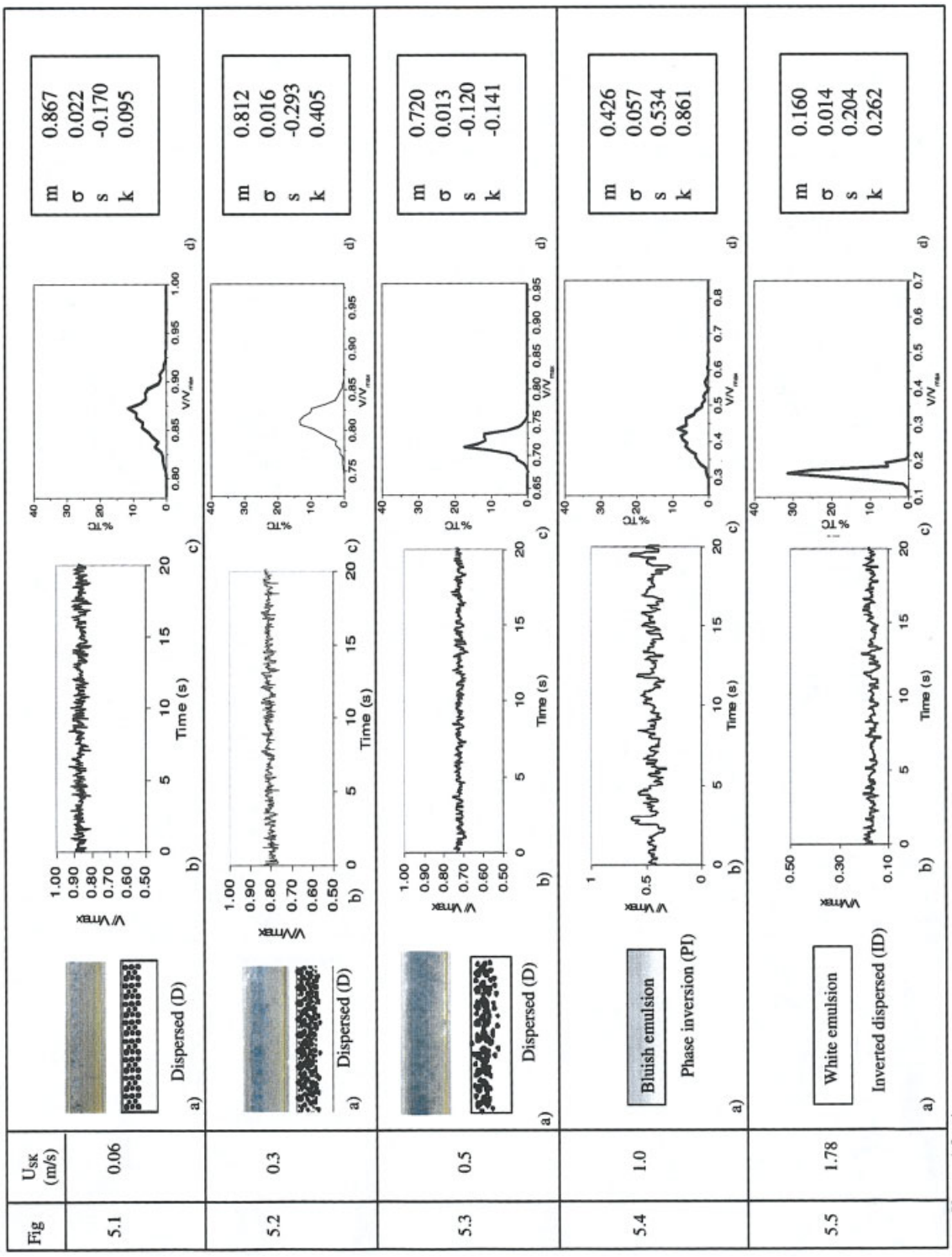

Figure 5. Visual and photographic observation, probe signal, and PDF curve for the different patterns at U_{SW} = 1.3 m/s.

[Color figure can be viewed in the online issue, which is available at www.interscience.wiley.com.]

to the spread at the other levels. This continues until the phase inversion point corresponding to Figure 5.4.

During phase inversion, the wavelet analysis presents certain interesting features. It is denoted by a remarkable increase of the spread at all levels from d_1-d_5 as well as the a_5 signal, as compared to the wavelet decompositions at lower oil velocities. Moreover, for lower oil velocities, the d_1 oscillations were observed to be the highest as compared to the other levels for a particular set of phase flow rates, On the other hand, the situation corresponding to Figure 5.4 (U_{SK} = 1m/s) is marked by an increase in the fluctuations from d_1-d_3 and a high value of the spread from d_3-d_5 and a_5 as compared to that for d_1. This shows that the increased PDF spread under these conditions is not due to an increase in the d_1 fluctuations only as has been observed in the previous cases. Rather, this is characterized by an increase in the variance at all levels of decomposition as

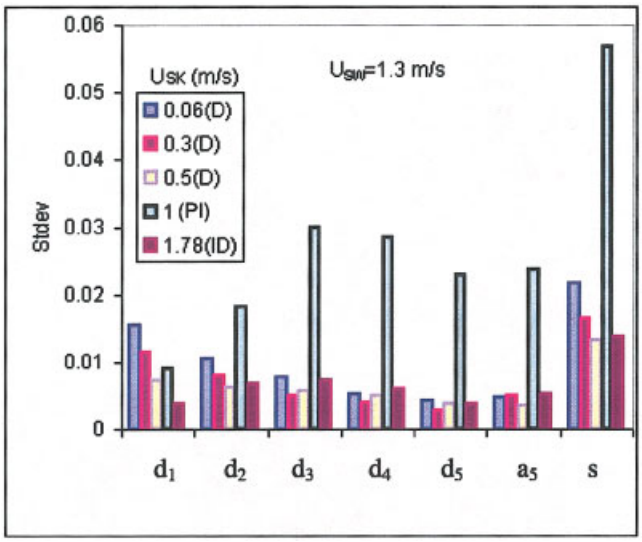

Figure 6. The spread at the different levels of the decomposed signal for USW = 1.3 m/s.

[Color figure can be viewed in the online issue, which is available at www.interscience.wiley.com.]

well as the a_5 signal, thus hinting at kerosene coalescence to form a continuous phase. It can, therefore, be deduced that the onset of inversion occurs due to the coalescence of the dispersed phase and is marked by a random distribution of the two liquids with a continually changing interface.

At still higher kerosene velocities, the fluctuations at all levels reduce but the magnitude of spread increases slightly from d_1-d_3. This shows that the flow has entered the oil predominant regime. Thus, Figure 6 distinguishes between the oil dispersed and the water dispersed flow patterns from the fluctuations at the different levels of the decomposed signal and its approximation and shows that the coalescence of oil droplets brings about phase inversion.

The distribution of water in oil at high kerosene velocities

An interest was next felt to understand the phase distribution when oil is the major phase in the conduit. For this, the experiments have been performed for increasing water velocities at different constant flow rates of oil. The flow rates have been selected such that the oil phase is the predominant phase under all conditions. The results have been represented in a tabular form for one oil velocity (U_{SK} = 1.78 m/s) in Figure 7. The rows of the figure, numbered as 7.1, 7.2, and so on, represent the situation with increasing water velocity. They present the visual appearance of the flow along with the probe signals, PDF curves, and the PDF moments for specific flow rates of the two phases.

From the figure, it is evident that at low water velocities, the flow passage appears to be hazy with kerosene flowing as a continuous medium and water droplets clinging to the lower portion of the pipe. The probe signals show random oscillations and the PDF is smooth and unimodal.

An increase in water velocity brings about an increase in the oscillations of the response, with the oscillations pointing towards the higher voltage values. The PDF curve shifts to V/Vmax $<$ 0.5. It is characterized by an increased spread and a positive skewness. It may be noted that an identical situation (breakdown in the smoothness of the PDF curve and the change in skewness) was noted during plug flow in Figure 3.

A subsequent increase of water velocity shifts the peak to still lower values of V/Vmax, accompanied by a decrease in the spread and the renewal of a smooth PDF curve (Figure 7.4) with a positive value of skewness. A similar observation is noted during dispersed flow in Figure 3 and can be attributed to the increased effect of light scattering by the dispersion. This, therefore, suggests the presence of a continuous kerosene phase with a water-in-oil type of distribution.

The wavelet analysis for the different probe signals presented in Figure 7 is shown in Figure 8. The figure indicates the spread at the different levels of the decomposed signal (d1-d5) and its approximation (a5) as a function of water superficial velocity. A comparison of Figures 4 and 8 clearly brings out the differences in the nature of the curves obtained for the water continuous and the oil continuous regions. Figure 8 also shows that the large spread in Figure 7.2c arises due to the continuous increase in fluctuations at all levels of the decomposed signal.

The aforementioned discussion suggests that water is probably dispersed in oil under these conditions. However, an additional check was felt necessary to ascertain the fact and rule out the possibilities of a separated flow pattern.

The sampling technique to understand the distribution of water in oil

Keeping the above in mind, a sampling technique has been devised to estimate the distribution of water in the continuous oil phase. For this, three sampling syringes, each with 20 ml capacity, are installed in the test rig beside the optical probe. Syringes A and B are connected to the top and bottom wall of the pipe, while syringe C is installed to draw the two phase mixture from the pipe center, as shown in Figure 9. Syringes A and B are located at diametrically opposite points, and syringe C is located at a distance of 10 cm from A. It is ensured that syringes A and B are flush mounted with the tube wall to minimize disturbance of flow. The two-phase mixture is drawn simultaneously through the three syringes for all the flow conditions depicted in Figure 7 and allowed to settle. The proportion of the two liquids is noted after gravity separation. The results are presented in Table 2. The table indicates that at low water velocities (Figures 7.1 and 7.2), water exists at the bottom of the pipe and a uniform emulsion of the two results at high phase velocities. Accordingly, the situation in Figure 7.1 is designated as oil and water in oil flow. Figure 7.2 denotes a situation similar to the plug flow pattern. Therefore, this distribution is designated as inverted plug flow, with kerosene as the continuous phase and intermittent water as chunks at the bottom wall. Such a pattern has not been reported for gas liquid systems. In order to distinguish the dispersion at high oil velocities from oil dispersed in water flow, this pattern is designated as the inverted dispersed flow pattern.

The flow pattern map to denote phase inversion

The results of the aforementioned experiments have been represented in the form of a flow pattern map in Figure 10, where the input proportion of oil (β) is plotted as a function of

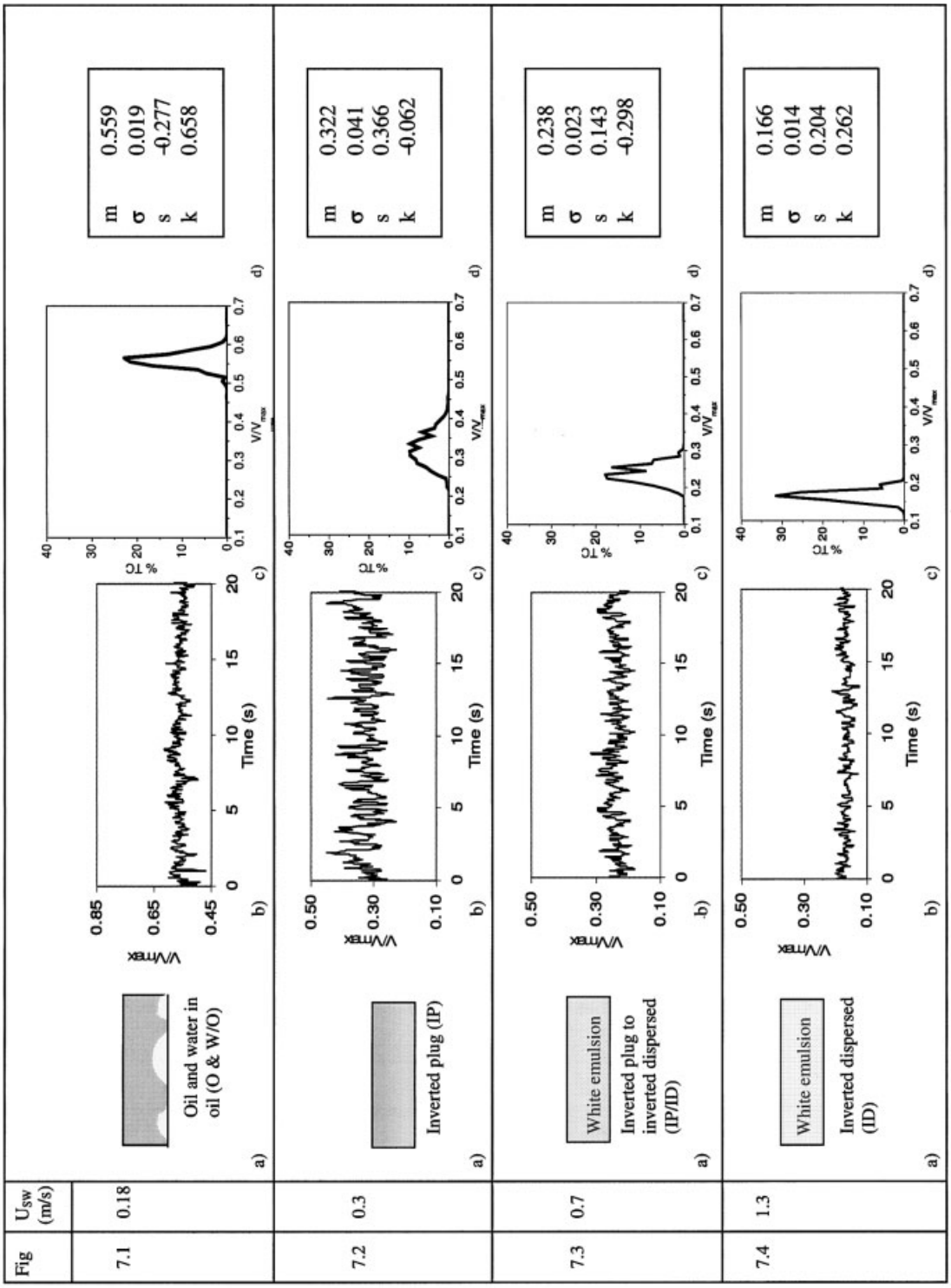

Figure 7. Schematic diagram, probe signal, PDF, and PDF moments of the different flow patterns at U_{SK} = 1.78 m/s.

the mixture velocity U_M (U_{SW} + U_{SK}). The figure shows that the flow exists as oil droplets dispersed in water at low oil input fractions (denoted as curve A in Figure 10) and water dispersed in oil (curve B) at high oil input for a constant mixture velocity. In the region between the two curves, there is a random mixture of the two liquids in which the dispersed phase gradually coalesces to form the continuous phase with change of fluid velocities. This is termed as the ambivalent range, which is marked by coalescence of the dispersed phase, a random mixture of the two liquids, and a continually changing interface.

It can be observed that curves A and B (when produced) appear to meet at a point. This shows that the range of the ambivalent region reduces with increasing mixture velocities; and at very high phase flow rates, the change from dispersed to inverted dispersed flow is expected to occur spontaneously. An identical observation has been reported by Tidhar et al.[7] for

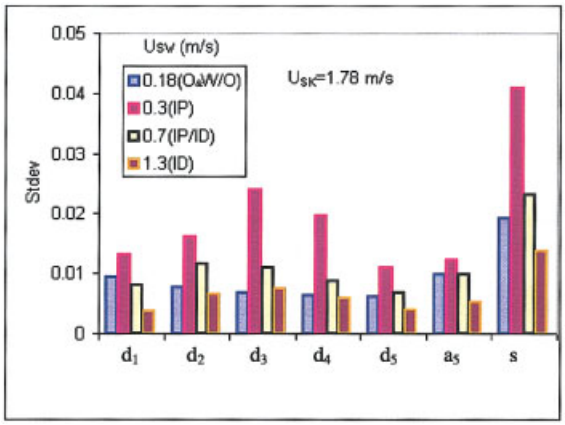

Figure 8. Change of standard deviation with different levels of the decomposed signal at USK = 1.78 m/s.

[Color figure can be viewed in the online issue, which is available at www.interscience.wiley.com.]

different pairs of liquids flowing in a motionless mixer where they plotted the oil fraction as a function of the Weber number.

Comparison of the flow pattern map with results from literature

The flow pattern map thus obtained is compared with the equations reported in the literature to predict phase inversion. The empirical equations to predict inversion have been proposed by Arirachakaran et al.[5] and Yeh et al.[6]

The empirical model suggested by Arirachakaran et al.[5] states that:

$$\varepsilon_w^1 = \left(\frac{U_{ws}}{U_m}\right) = 0.5 - 0.1108 \log_{10}\left(\frac{\eta_o}{\eta_w}\right) \quad (1)$$

where $\varepsilon_w{}^1$ is the critical water cut for phase inversion, and η_w and η_o are the water and oil viscosity. U_{ws} and U_m represent the water and mixture superficial velocities, respectively.
The model proposed by Yeh et al.[6] states:

$$\varepsilon_w^I = 1/(1 + (\eta_o/\eta_w)^{0.5}) \quad (2)$$

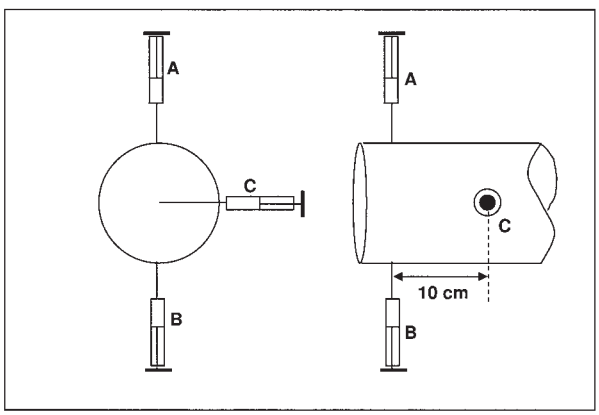

Figure 9. Sampling technique in the pipe.

Table 2. Composition of Two Phase Mixture as Obtained from the Sampling Probe

	Fraction of Water at U_{SK} = 1.78 m/s From Syringe		
U_{SW} (m/s)	(A) Top	(C) Center	(B) Bottom
0.18	0.00	0.00	0.10
0.3	0.00	0.00	0.45
0.7	0.02	0.09	0.69
1.3	0.32	0.35	0.43

Both equations have been superimposed in the flow pattern map as curves C and D in Figure 11. The figure shows that the equations predict straight lines, which lie in the ambivalent region. They indicate that phase inversion is independent of oil input fraction, which is true at high mixture velocities. Curve D due to Yeh et al.[6] appears to be closer to the point of intersection of the extrapolations of curves A and B (when produced).

Tidhar et al.[7] have suggested phase inversion to occur at the point where the surface energies of the two possible dispersions (oil dispersed in water and water dispersed in oil) are equal. This has been used with considerable success by Brauner and Ullmann[9] for liquid-liquid flow through horizontal pipes. The model also predicts a single curve close to curve D. This has been represented as curve E in Figure 11.

Attempts have next been made to superimpose the onset of dispersed flows as predicted by Brauner[34] in the map. The transition to dispersed oil in water and dispersed water in oil patterns from the mixed stratified pattern is based on the postulation that a homogeneous dispersion can be maintained when the turbulence level in the continuous phase is sufficiently high. The continuous phase disperses the second phase into small and stable droplets of a maximum diameter, d_{max}, which is less than the critical diameter, d_{crit}, where d_{crit} is obtained from:

$$\frac{d_{crit}}{D} = \mathrm{Min}\left(\frac{d_{c\sigma}}{D}, \frac{d_{cb}}{D}\right) \quad (3)$$

In Eq. 3, $d_{c\sigma}$ represents the maximal drop diameter above which drops are deformed, and d_{cb} represents the maximal drop

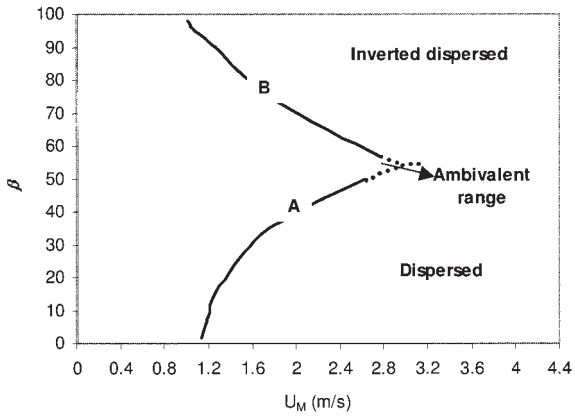

Figure 10. Flow pattern map for the transition from the water continuous to the oil continuous regime.

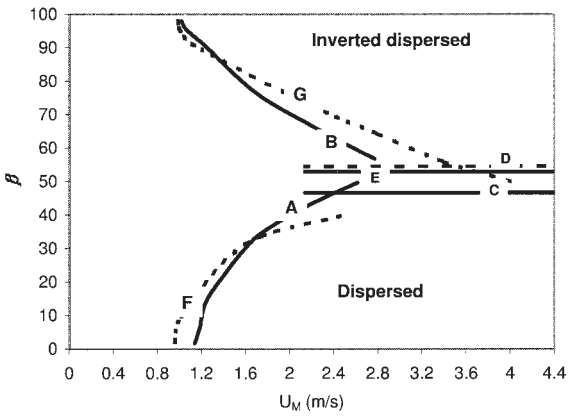

Figure 11. A comparison of the present map with results of literature.

diameter above which drops would go to the wall due to buoyancy.

The transitions have been represented as curves F and G in Figure 8 for oil and water dispersion, respectively, and are calculated from the extended Hinze model (H-model[34]). They are observed to lie close to the predictions of the present work.

Conclusion

In the present study, an effort has been made to develop an objective indicator for phase inversion during liquid-liquid flow through horizontal pipes. The random signals from a novel optical probe and their statistical analysis (probability density function analysis and the wavelet multiresolution technique) have been adopted for this purpose. The indicator denotes the distribution to invert from an oil in water dispersion to water in oil dispersion when the PDF shifts to V/Vmax <0.5 and the skewness changes sign. The PDF spread is also maximum under these conditions. The study has also revealed the presence of inverted plug flow and inverted dispersed flow when the oil is the predominant liquid in the conduit. The ambivalent range as predicted in the present study is in close agreement to the results reported in literature.

Literature Cited

1. Angeli P, Hewitt GF. Pressure gradient in horizontal liquid-liquid flows. *Int J Multiphase Flow*. 1998;24:1183-1203.
2. Selker AH, Sleicher Jr CA. Factors affecting which phase will disperse when immiscible liquids are stirred together. *Canadian J Chem Eng.* 1965;43:298-301.
3. Norato MA, Tsouris C, Tavlarides LL. Phase inversion studies in liquid-liquid dispersions. *Canadian J Chem Eng.* 1998;76:486-494.
4. Zaldivar JM, Alos MA, Molga E, Hernandez H, Westerterp KR. The effect of phase inversion during semibatch aromatic nitrations. *Chem Eng Proc*. 34;1995: 529-542.
5. Arirachakaran S, Oglesby KD, Malinowsky MS, Shoham O, Brill JP. An analysis of oil/water flow phenomena in horizontal pipes. In: SPE Paper 18836, SPE Prod Operating Symp, held in Oklahoma City, OK, March 13-14, 1989:155-167.
6. Yeh G, Haynie Jr., FH, Moses RE. Phase-volume relationship at the point of phase inversion in liquid dispersions. *AIChE J.* 1964;102:260-265.
7. Tidhar M, Merchuk JC, Sembira AN, Wolf D. Characteristics of a motionless mixer for dispersion of immiscible fluids. II. Phase inversion of liquid–liquid systems. *Chem Eng Sci.* 1986;41:457-462.
8. Nädler M, Mewes D. The effect of gas injection on the flow of immiscible liquids in horizontal pipes. *Chem Eng Tech.* 1995;18:156-165.
9. Brauner N, Ullmann A. Modelling of phase inversion phenomenon in two-phase pipe flow. *Int J Multiphase Flow*. 2002;28:1177-1204.
10. Chesters AK, Issa R. A framework for the modelling of phase inversion in liquid-liquid systems. Paper No. 271, 5th Int Conf Multiphase Flow, ICMF'04, Yokohama, Japan, May 30-June 4, 2004.
11. Russell TWF, Charles ME. The effect of the less viscous liquid in the laminar flow of two immiscible liquids. *Canadian J Chem Eng.* 1959;37:18-24.
12. Charles ME, Govier GW, Hodgson GW. The horizontal pipeline flow of equal density oil-water mixture. *Canadian J Chem Eng.* 1961;39: 27-36.
13. Hasson D, Mann U, Nir A. Annular flow of two immiscible liquids. I. Mechanisms. *Canadian J Chem Eng.* 1970;48:514-520.
14. Guzhov A, Grishin AD, Medredev VF, Medredeva OP. Emulsion formation during the flow of two liquids in a pipe. Neft Khoz 1973;8: 58-61 (in Russian).
15. Vigneaux P, Chenais P, Hulin JP. Liquid-liquid flows in an inclined pipe. *AIChE J,*. 1988;34:781-789.
16. Angeli P, Hewitt GF. Flow structure in horizontal oil-water flow. *Int J Multiphase Flow*. 2000;26:1117-1140.
17. Jin ND, Nie XB, Ren YY, Liu XB. Characterization of oil/water two-phase flow patterns based on nonlinear time series analysis. *Flow Measurement Instrum.* 2003;14:169-175.
18. Lovick J, Angeli P. Experimental studies on the dual continuous flow pattern in oil–water flows. *Int J Multiphase Flow*. 2004;30:139-157.
19. Ioannou K. Hu B, Matar OK, Hewitt GF, Angeli P. Phase inversion in dispersed liquid-liquid pipe flows. Paper No. 108, 5th Int Conf Multiphase Flow, ICMF'04, Yokohama, Japan, May 30-June 4, 2004.
20. Ioannou K, Nydal OJ, Angeli P. Phase inversion in dispersed liquid–liquid flows. *Exp Therm Fluid Sci.* 2005;29:331-339.
21. Steinhauff E. Modern oil field demulsification: I. *Petrol.* 1962;25:294-298.
22. Alvarado DA, Marsden SS. Flow of oil-in-water emulsions through tubes and porous media. *SPEJ*. 1979;Dec:369-377.
23. Hapanowicz J, Troniewski L. Two-phase flow of liquid–liquid mixture in the range of the water droplet pattern. *Chem Eng Proc.* 2002;41: 165-172.
24. Raj TS, Chakrabarti DP, Das G. Liquid–liquid stratified flow through horizontal conduit. *Chem Eng Tech.* 2005;28:899-907.
25. Jana AK, Das G, Das PK. A novel technique to identify flow patterns during liquid-liquid two-phase upflow through vertical pipe, *Indus Eng Chem Res.* 2006;45:2381-2393.
26. Jana AK, Das G, Das PK. Flow regime identification of two-phase liquid-liquid upflow through vertical pipe. *Chem Eng Sci.* 2006;61: 1500-1515.
27. Drahos J, Cermak J. Diagnostics of gas-liquid patterns in chemical engineering systems. *Chem Eng Proc.* 1989;26:147-164.
28. Vince MA, Lahey Jr RT. On the development of an objective flow regime indicator. *Int J Multiphase Flow*. 1982;8:93-124.
29. Ren J, Mao Q, Li J, Lin W. Wavelet analysis of dynamic behaviour in fluidized beds. *Chem Eng Sci.* 2001;56:981-988.
30. Ellis N, Briens LA, Grace JR, Bi HT, Lim CJ. Characterization of dynamic behaviour in gas-solid turbulent fluidized bed using chaos and wavelet analyses. *Chem Eng J*. 2003;96:105-116.
31. Ellis N, Bi HT, Lim CJ, Grace JR. Influence of probe scale and analysis method on measured hydrodynamic properties of gas-fluidized beds. *Chem Eng Sci.* 2004;59:1841-1851.
32. Briens LA, Ellis N. Hydrodynamics of three-phase fluidized bed systems examined by statistical, fractal, chaos and wavelet analysis methods. *Chem Eng Sci.* 2005;60:6094-6106.
33. Drahos J, Ruzicka, MC. Problems of time series analysis in characterization of multiphase flows. Paper No. K04, 5th Int Conf Multiphase Flow, ICMF'04, Yokohama, Japan, May 30-June 4, 2004.
34. Brauner N. The prediction of dispersed flows boundaries in liquid-liquid and gas-liquid systems. *Int J Multiphase Flow*. 2001;27:885-910.

Manuscript received Apr. 26, 2006, and revision received July 19, 2006.